Interphase Cracking in Titanium Nitride/2024 Alloy Particle-Reinforced Metal-Matrix Composites

[1]B. Kotiveera Chari and A. Chennakesava Reddy[2]

[1]Professor, Department of Mechanical Engineering, N.I.T, Warangal, India
[2]Associate Professor, Department of Mechanical Engineering, Vasavi College of Engineering, Hyderabad, India
dr_acreddy@yahoo.com

Abstract: In the present work, the TiN/AA2024 alloy metal matrix composites were subjected to mechanical and thermal loads. The results obtained from the finite element analysis and experimental procedure of TiN/2024 alloy composites reveal the interphase separation from the particle and the matrix.

Keywords: Titanium nitride, AA2024 alloy, RVE model, finite element analysis, interphase separation.

1. INTRODUCTION

The ceramic particle-reinforced metal matrix composite (PMMC) has been widely paid great attention to on its high strength. a lot of researches on the mechanical properties of the PMMC have been done. In experimental researches, the effects of particle size and particle volume fraction on the strength have studied. It has been reported that the strength increases with particle volume fraction and it decreases with increase of particle size. The effect of weak bonding or debonded interface on the mechanical properties has been studied by several investigators using simplified models for representing imperfect conditions through traction discontinuities [1, 2]. A majority of the studies have used unit cell models [3, 4], which assume that the material is constituted of periodic repetition of single cells 5-18]. Displacement based finite element analyses, with the inclusion-matrix interface represented through traction displacement constitutive models, is used to predict the onset and growth of debonding.

The objective of the present paper was to evaluate the effect of thermo-mechanical loading on the interphase separation in titanium nitride/AA2024 alloy composites. The shape of titanium nitride nanoparticle considered in this work is spherical. The periodic particle distribution was a square array and corresponding representative volume element (RVE) is showed in figure 1.

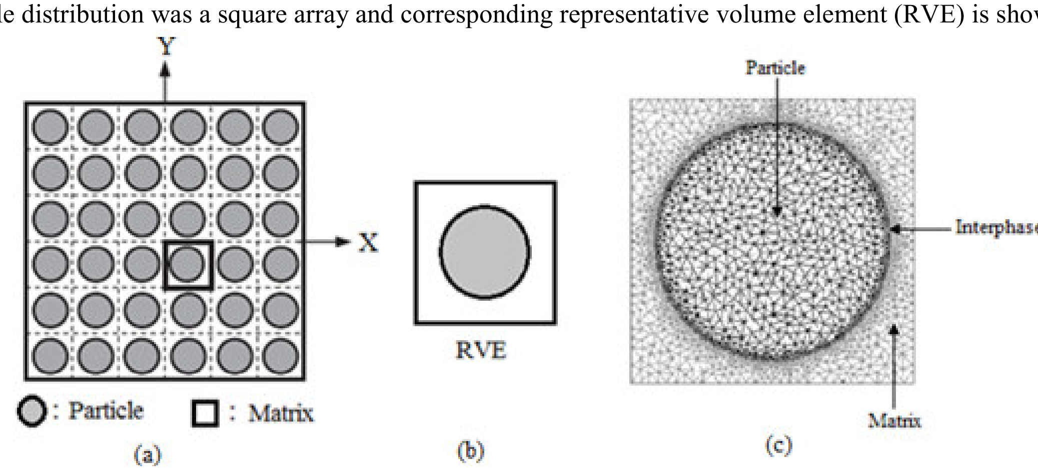

Figure 1: Square array of particles (a); Representative Volume Element (b); and Discretization of RVE (c).

Table 1: Mechanical properties of AA2024 matrix and TiN nanoparticles

Property	AA2024	TiN
Density, g/cc	2.8	5.22
Elastic modulus, GPa	72.4	251.0
Coefficient of thermal expansion, 10^{-6} 1/^{o}C	20.8	9.35
Specific heat capacity, J/kg/^{o}C	880	757
Thermal conductivity, W/m/^{o}C	134	19.2
Poisson’s ratio	0.33	0.19

2. MATERIALS METHODS

The matrix material was AA2024 alloy. The reinforcement material was titanium nitride (TiN) nanoparticles of average size 100nm. The mechanical properties of materials used in the present work are given in table 1.

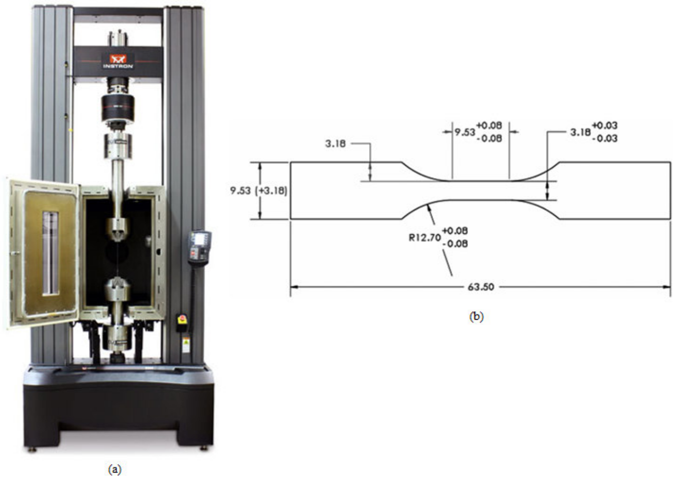

Figure 2: Tensile testing: UTM with temperature controlled chamber and (b) shape and dimensions of tensile specimen.

TiN/AA2024 alloy composites were fabricated by the stir casting process and low pressure casting technique with argon gas at 3.0 bar. The composite samples were give solution treatment and cold rolled to the predefined size of tensile specimens. The heat-treated samples were machined to get flat-rectangular specimens (figure 2) for the tensile tests. The tensile specimens were placed in the grips of a Universal Test Machine (UTM) with temperature controlled chamber at a specified grip separation and pulled until failure. The test speed was 2 mm/min. A strain gauge was used to determine elongation. In the current work, a cubical representative volume element (RVE) was implemented to analyze the tensile behavior TiN/AA2024 alloy composites at two (10% and 30%) volume fractions of TiN and at different temperatures. The large strain PLANE183 element was used in the matrix in all the models. In order to model the adhesion between the matrix and the particle, a CONTACT 172 element was used.

3. RESULTS AND DISCUSSION

The optical micrograph as shown in figure 3 reveals random distribution of TiN particles in AA2024 alloy matrix. Agglomeration of TiN particles is also revealed in the microstructures.

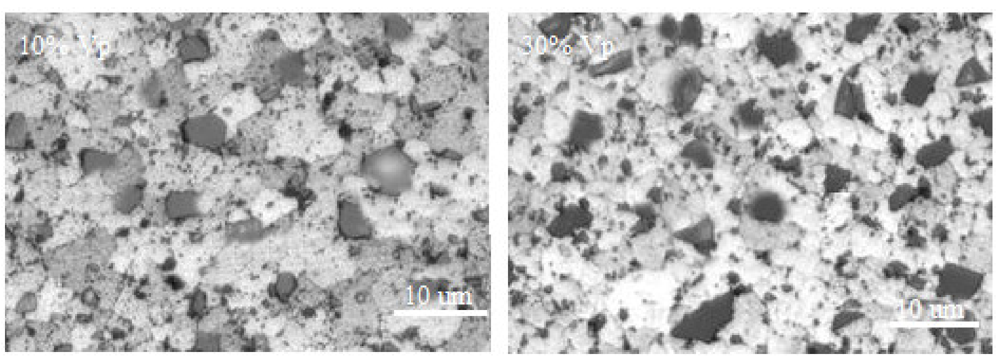

Figure 3: Microstructure showing distribution of TiN nanoparticles in AA2024 alloy matrix.

3.1 Thermo-Mechanical Behavior

Figure 4a shows the normalized elastic modulus of TiN/AA2024 composites at different temperatures. The elastic modulus is normalized with the elastic modulus of AA2024 alloy. When the temperature is increased from 30°C to 300°C, the normalized elastic modulus is decreased. Under thermo-mechanical loading, the stiffness of 30% TiN/AA2024 alloy composites is lower than that of 10% TiN/AA2024 alloy composites because of the difference in thermal properties of TiN and AA2024 alloy. The normalized stiffness along the normal direction is lower than that along the load direction owing to tensile loading consideration in the present work. The normalized shear modulus is unchanged with increase of temperature as shown in figure 4b. For the increase of temperature from 100^{o}C to 300^{o}C, the increase of major Poisson's ratio (figure 4c) indicates the elongation along the load is greater than that along the transverse direction of loading of RVE.

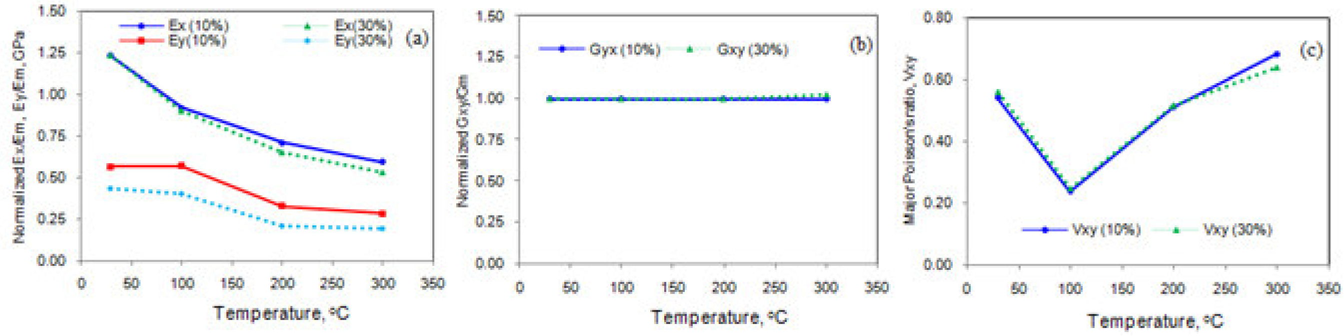

Figure 4: Effect of temperature on micromechanical properties of TiN/AA2024 composites.

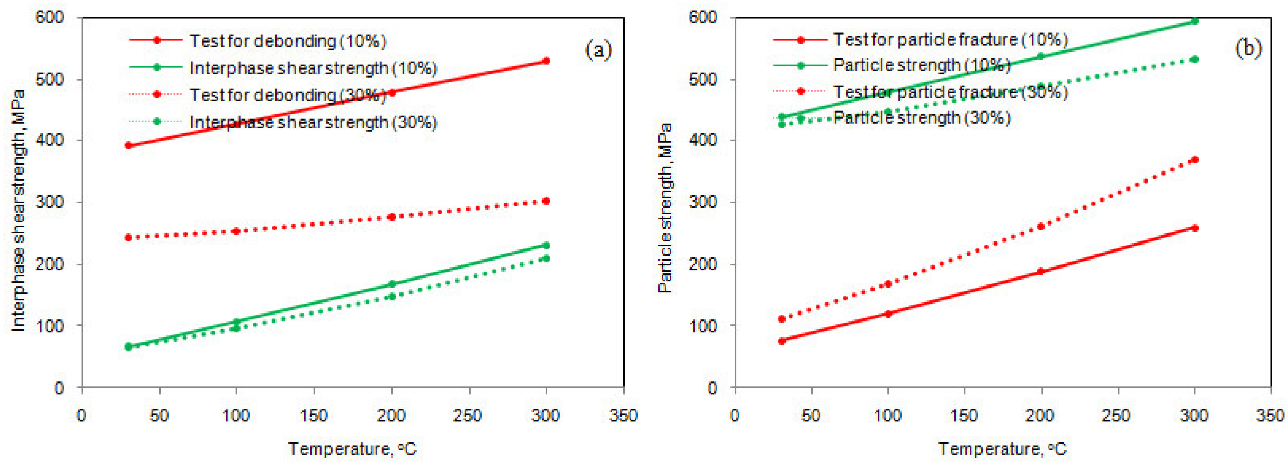

Figure 5: Criterion for interfacial debonding (a) and for particle fracture (b).

3.2 Fracture Behavior

If the particle deforms in an elastic manner (according to Hooke's law) then,

$$\tau = \frac{n}{2}\sigma_p \quad (1)$$

where σ_p is the particle stress. For the interfacial debonding/yielding to occur, the interfacial shear stress reaches its shear strength:

$$\tau = \tau_{max} \quad (2)$$

For particle/matrix interfacial debonding can occur if the following condition is satisfied:

$$\tau_{max} < \frac{n\sigma_p}{2} \quad (3)$$

It is observed from figure 5a that the interphase debonding occurs between TiN nanoparticle and AA2024 alloy matrix as the condition in Eq.(3) is satisfied. The normal displacement field (figure 6) across the interphase increases with increase of temperature. This confirms the increase of interphase separation from TiN particle and AA2024 alloy matrix with increase of temperature. Further, the normal and tangential tractions (figure 7) along the interphase increase with increase of temperature to take place the interphase separation from TiN particle and AA2024 alloy matrix.

If particle fracture occurs when the stress in the particle reaches its ultimate tensile strength, $\sigma_{p,uts}$, then setting the boundary condition at

$$\sigma_p = \sigma_{p,\,uts} \quad (4)$$

The relationship between the strength of the particle and the interfacial shear stress is such that if

$$\sigma_{P,uts} < \frac{2\tau}{n} \quad (5)$$

Then the particle will fracture. From the figure 5b, it is observed that the TiN nanoparticle was not fractured as the condition in Eq. (5) is not satisfied.

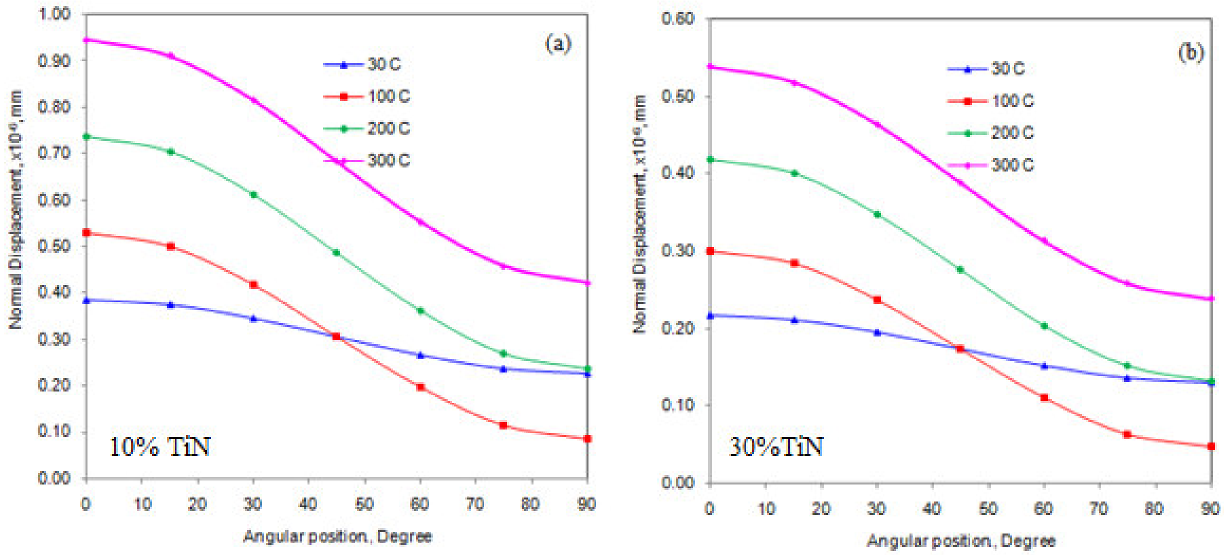

Figure 6: Normal displacement across the interphase between TiN particle and AA2024 alloy matrix.

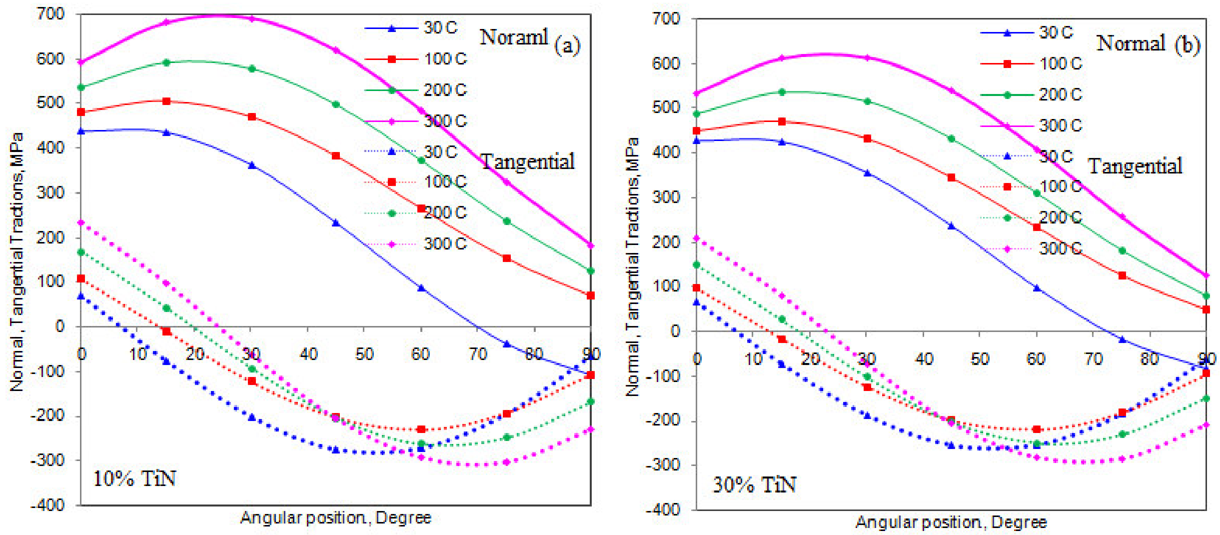

Figure 7: Normal and tangential tractions along the interphase.

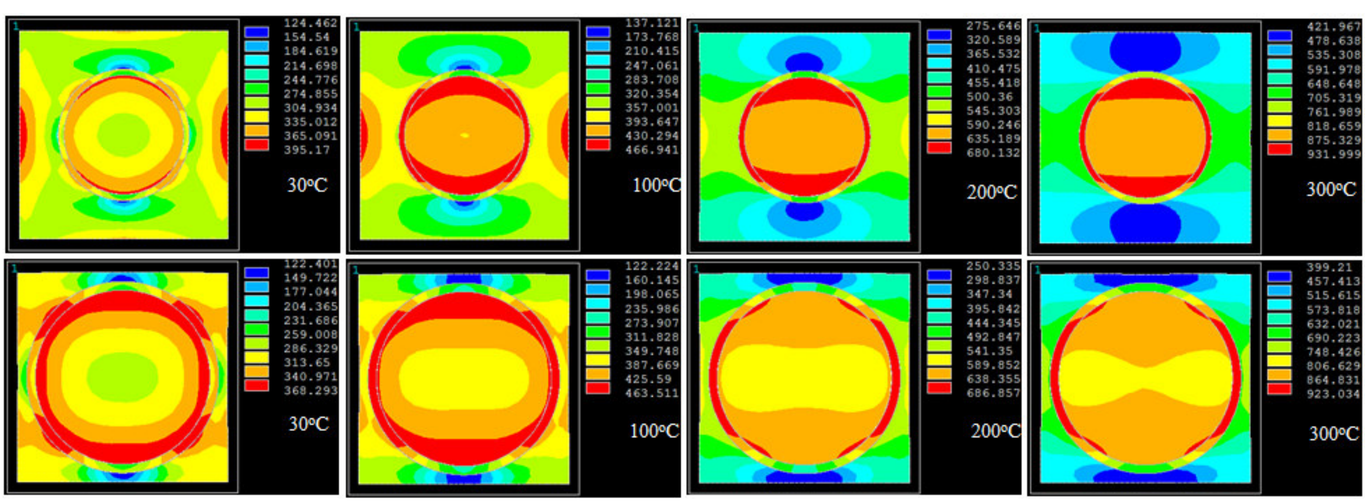

Figure 8: Images of von Mises stresses obtained from FEA: (a) 10%TiN/AA2024 alloy and (b) 30%TiN/AA2024 alloy composites.

The von Mises stress as a function of temperature is illustrated in figure 8. The von Mises stresses induced at the interface are higher than that induced in the nanoparticle. Hence, the interphase separation has occurred between the particle and the matrix. The particle fracture was not occurred in TiN/AA2024 alloy composites as the stress induced in the TiN particle does not exceed its allowable stress due to thermal shock. The scanning electron micrograph (figure 9) of 30%TiN/AA2024 alloy composite confirms the absence of particle fracture.

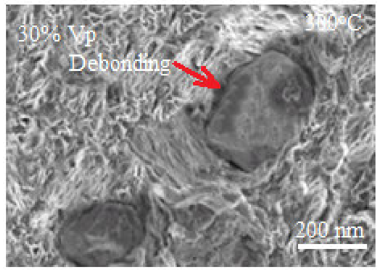

Figure 9: SEM illustrating the interphase separation.

4. CONCLUSION

The microstructure of TiN/AA2024 alloy composites reveals random uniform distribution of TiN nanoparticles in AA2024 alloy. The shear stress is high at the interface resulting to interphase separation from the particle and the matrix. The interphase separation has occurred between the particle and the matrix.

REFERENCES

1. Y. Benveniste, On the effect of debonding on the overall behavior of composite materials, Mechanics of Materials, 3, 1984, pp. 349-358.
2. N. J. Pagano, G. P. Tandon, Modeling of imperfect bonding in fiber reinforced brittle matrix composites, Mechanics of Materials, 9, 1990, pp. 49-64.
3. D. C. Lo, D.H. Allen, Modeling of delamination damage evolution on laminated composites subjected to low velocity impact, International Journal of Damage, 3, 1994, pp.378-407.
4. M. E. Walter, G. Ravichandran, M. Ortiz, Computational modeling of damage evolution in unidirectional fiber-reinforced ceramic-matrix composites, Computational Mechanics, 20, 1997, pp. 192-198.
5. A. Chennakesava Reddy, Evaluation of Debonding and Dislocation Occurrences in Rhombus Silicon Nitride Particulate/AA4015 Alloy Metal Matrix Composites, 1st National Conference on Modern Materials and Manufacturing, Pune, India, 19-20 December 1997, pp. 278-282.
6. A. Chennakesava Reddy, Interfacial Debonding Analysis in Terms of Interfacial Tractions for Titanium Boride/AA3003 Alloy Metal Matrix Composites, 1st National Conference on Modern Materials and Manufacturing , Pune, 19-20 December, 1997.
7. A. Chennakesava Reddy, Assessment of Debonding and Particulate Fracture Occurrences in Circular Silicon Nitride Particulate/AA5050 Alloy Metal Matrix Composites , National Conference on Materials and Manufacturing Processes, Hyderabad, India, 27-28 February 1998, pp. 104-109.
8. A. Chennakesava Reddy, Local Stress Differential for Particulate Fracture in AA2024/Titanium Carbide Nanoparticulate Metal Matrix Composites, National Conference on Materials and Manufacturing Processes, Hyderabad, India, 27-28 February 1998, pp. 127-131.
9. A. Chennakesava Reddy, Micromechanical Modelling of Interfacial Debonding in AA1100/Graphite Nanoparticulate Reinforced Metal Matrix Composites, 2nd International Conference on Composite Materials and Characterization, Nagpur, India, 9-10 April 1999, pp. 249-253.
10. A. Chennakesava Reddy, Cohesive Zone Finite Element Analysis to Envisage Interface Debonding in AA7020/Titanium Oxide Nanoparticulate Metal Matrix Composites, 2nd International Conference on Composite Materials and Characterization, Nagpur, India, 9-10 April 1999, pp. 204-209.
11. H. B. Niranjan, A. Chennakesava Reddy, Computational Modeling of Interfacial Debonding in Fused Silica/AA7020 Alloy Particle-Reinforced Metal Matrix Composites, 3rd International Conference on Composite Materials and Characterization, Chennai, India, 11-12 May 2001, pp. 222-227.
12. H. B. Niranjan, A. Chennakesava Reddy, Nanoscale Characterization of Interfacial Debonding and Matrix Damage in Titanium Carbide/AA8090 Alloy Particle-Reinforced Metal Matrix Composites, 3rd International Conference on Composite Materials and Characterization, Chennai, India, 11-12 May 2001, pp. 228-233.
13. S. Sundara Rajan, A. Chennakesava Reddy, Assessment of Temperature Induced Fracture in Boron Nitride/AA1100 Alloy Particle-Reinforced Metal Matrix Composites, 3rd International Conference on Composite Materials and Characterization, Chennai, India, 11-12 May 2001, pp. 234-239.
14. S. Sundara Rajan, A. Chennakesava Reddy, Estimation of Fracture in Zirconia/AA2024 Alloy Particle-Reinforced Composites Subjected to Thermo-Mechanical Loading, 3rd International Conference on Composite Materials and Characterization, Chennai, India, 11-12 May 2001, pp. 240-245.

15. P. M. Jebaraj, A. Chennakesava Reddy, Finite Element Predictions for the Thermoelastic Properties and Interphase Fracture of Titanium Nitride /AA3003 Alloy Particle-Reinforced Composites, 3rd International Conference on Composite Materials and Characterization, Chennai, India, 11-12 May 2001, pp. 246-251.
16. P. M. Jebaraj, A. Chennakesava Reddy, Effect of Thermo-Mechanical Loading on Interphase and Particle Fractures of Titanium Oxide /AA4015 Alloy Particle-Reinforced Composites, 3rd International Conference on Composite Materials and Characterization, Chennai, India, 11-12 May 2001, pp. 252-256.
17. A. Chennakesava Reddy, Effect of CTE and Stiffness Mismatches on Interphase and Particle Fractures of Zirconium Carbide /AA5050 Alloy Particle-Reinforced Composites, 3rd International Conference on Composite Materials and Characterization, Chennai, India, 11-12 May 2001, pp. 257-262.
18. A. Chennakesava Reddy, Behavioral Characteristics of Graphite /AA6061 Alloy Particle-Reinforced Metal Matrix Composites, 3rd International Conference on Composite Materials and Characterization, Chennai, India, 11-12 May 2001, pp. 263-269.